View Article Online / Journal Homepage / Table of Contents for this issue

Synthesis of $Co_3[Fe(CN)_6]_2$ molecular-based nanomagnets in MSU mesoporous silica by integrative chemistry†

Rola Mouawia,[a] Joulia Larionova,*[b] Yannick Guari,[b] Seungwon Oh,[a] Phil Cook[a] and Eric Prouzet*[a]

Received (in Montpellier, France) 19th June 2009, Accepted 5th August 2009
First published as an Advance Article on the web 22nd September 2009
DOI: 10.1039/b9nj00271e

Published on 22 September 2009 on http://pubs.rsc.org | doi:10.1039/B9NJ00271E
Downloaded by University of Belgrade on 02 January 2013

Nanometric particles of $Co_3[Fe(CN)_6]_2$ magnetic cyano-bridged polymers have been synthesised by the combination of the direct synthesis of mesoporous MSU-type silica and the parallel reaction of cobalt nitrate with potassium ferricyanide. This synthesis, relevant to integrative chemistry methods, allowed us to confine the particle growth during the building of the mesostructured framework of silica. The obtained composite materials were studied by XRD, SAXS, TEM and FT-IR. Magnetic measurements of the nanoparticles extracted after silica dissolution by HF treatment, confirmed the expected magnetic behaviour of these Prussian Blue analogues. Compared with bulk materials, a spin-glass like regime is observed due to the presence of strong interparticle magnetostatic interactions between the nanoparticles which appeared as a result of the high density of nanoparticles in the nanocomposite materials synthesised by this new method.

Introduction

Molecular-based magnets, and among them Prussian blue analogues (PBA), are materials that exhibit adjustable properties (magnetic, optic, photo-switchable) based on their molecular structure and the possibility to modify them by the correct design of molecular entities where magnetic interactions between two different metal centres are controlled by the interatomic distance *via* a molecular connector such as a cyano-bridge.[1] Beyond the huge development of this class of compounds, a recent trend in research in this domain has been to generate small particles that could combine magnetic behaviour and nanometric-dependent properties. Since the first synthesis of Prussian blue nanocrystals in a reverse microemulsion,[2] there have been numerous methods investigated, based on reverse micelles,[3] polymers,[4] ionic liquids[5] or porous silica.[6]

Among the different methods of synthesis of nanoparticles, the use of a porous rigid matrix that will limit the growth of particles nucleated inside has been widely explored. This method was defined as nanocasting.[7] One of its drawbacks lies in the possibility to achieve the reaction inside the porous framework and avoid it outside. A recent study by Folch *et al.* reported a smart solution that allowed them to prepare cyano-bridged polymer nanoparticles with the general formula $M^{n+}/[M'(CN)_m]^{x-}$ inside SBA-15 or MCM-41 mesoporous silica. To avoid any reaction outside the internal porous structure, the silica was functionalized beforehand by $-(CH_2)_2C_5H_4N$ pyridine groups that allowed a selective anchorage of M^{n+} cations and avoided any segregation in excess of these cations. They could react in a second step with the metallo-cyano entities, the initial grafting density being the limiting factor for the particle growth along with the confinement provided by the porous framework. Despite its great success, this method still has some drawbacks: it requires a multistep process that starts with the initial grafting of pyridine, its metal complexation *via* a succession of impregnations and washing, and the final reaction of the metal cyano-complexes by similar impregnation and washing. In addition, a limited quantity of the nanoparticles (around 3–5%) may be inserted into the silica pores due to the limited quantity of the pyridine groups that can be grafted.

It has been pointed out recently that new chemical methods could take advantage of an integration of different shaping processes that combine sol–gel and/or soft chemistry techniques with the self-assembly mechanism of soft matter, potentially helped by chemical engineering processes. This emerging field was baptised "Integrative Chemistry".[8] We illustrate in the present report such a process by the integration of different mechanisms in a one-step process that allowed us to prepare directly nanoparticles of $Co_3[Fe_2(CN)_6]_2$ molecular magnets inside a matrix of MSU-type mesoporous silica. Synthesis of MSU mesoporous silica is achieved *via* a two-step process where stable hybrid micelles made of nonionic

[a] *University of Waterloo, Chemistry Dept & Institute of Nanotechnology, 200 University Av., W (ON) N2L 3G1, Canada. E-mail: eprouzet@scimail.uwaterloo.ca; Fax: +1 519 746-0435; Tel: +1 519 888-4567 x38172*
[b] *Institut Charles Gerhardt Montpellier, UMR 5253 CNRS-UM2-ENSCM-UM1, Chimie Moléculaire et Organisation du Solide, Université Montpellier II, Place E. Bataillon, F-34095 Montpellier Cedex 5, France. E-mail: joulia.larionova@univ-montp2.fr; Fax: +33 467-143-852*

† Electronic supplementary information (ESI) available: SI 1: FT-IR spectrum of (a) the bulk sample of $Co_3[Fe(CN)_6]_2$, and (b) the initial reagent $K_3Fe(CN)_6$. SI 2: EDAX analysis of samples B. SI 3: EDAX analysis of sample C. SI 4: Field-cooled and zero field-cooled magnetisation (FC/ZFC) *vs.* temperature curves performed with an applied field of 10 Oe for sample B; inset: field dependence of the magnetisation for sample B performed at 2 K. See DOI: 10.1039/b9nj00271e

Published on 22 September 2009 on http://pubs.rsc.org | doi:10.1039/B9NJ00271E
Downloaded by University of Belgrade on 02 January 2013

surfactants surrounded by a diffuse layer of silicate oligomers interacting with the palisade of polyethylene oxide chains, are created first.[9] These "hybrid micelles" can be either further destabilised by the addition of a fluoride salt that initiates the condensation of silicate oligomers, or they can be concentrated by simple evaporation. In the first process, micrometric spherical particles of mesoporous silica are obtained,[10] whereas evaporation leads to a spontaneous reaction giving a gel instead of particles. Additionally, the concentration operation is a way to trap hetero-species such as metal ions or particles with a high initial homogeneity, since the process occurs in the liquid state, which leads to a good distribution of species in the final material. We denote this process as hybrid micelle concentration (HMC). This HMC method was initially illustrated with the synthesis of Al-doped silica with a content of aluminium that could be easily adjusted using this method.[11]

We illustrate in the following how the HMC process can be used to combine the synthesis of PBA particles along with the synthesis of mesoporous silica. The current synthesis reported here combines two reactions: (i) the synthesis of PBA particles and (ii) the parallel synthesis of the mesostructured silica that will help to confine the PBA particle growth within the nanometer range. This method is fully relevant to Integrative Chemistry since the final material is obtained *via* a synergistic mechanism.[8] We report the single-step synthesis of PBA nanoparticles, generated in parallel with the reaction of a mesostructured silica framework, that ensures a confinement mechanism controlling the final size dispersion of molecular magnets.

Experimental

Chemicals

The nonionic PEO-based surfactant Brij 98, potassium hexacyanoferrate(III) ($K_3[Fe(CN)_6]$), cobalt(II) nitrate ($Co(NO_3)_2{\cdot}6H_2O$), and tetraorthosilicate (TEOS: $Si(OCH_2CH_3)_4$) were purchased from Sigma Aldrich and used as received.

Synthesis

MSU silica (sample A). A typical synthesis of MSU silica prepared with a Si/surfactant molar ratio of 20. A 0.1 mol L^{-1} solution of Brij 98 ($C_{18}H_{35}(OCH_2CH_2)_{\sim 20}OH$) was prepared by dissolution of 11.5 g into 100 mL of deionized water of pH = 2 and 41.4 g of TEOS was slowly added under magnetic stirring. A cloudy emulsion was obtained, which became clear within 15 min, after the total hydrolysis of TEOS. The mild acidity of the aqueous solution prevented the silica from precipitating. A rotary evaporator under dynamic primary vacuum and a heating bath set at 30 °C was used to remove 60–70% of the total mass, which included most of the ethanol generated by the TEOS hydrolysis. The solution was removed and left to gel for 48 h in a thermostated shaking bath. After completion of the condensation, the solid was collected, ground and surfactants were washed out by ethanol.

Nanocomposite prepared by double impregnation (sample B). For comparison, we prepared a sample by simple impregnation of the mesoporous silica prepared according to the previous method and further impregnated by precursors of PBA. This was achieved by means of incipient wetness with a reaction based on methods already reported.[12] The metal salts were dissolved in the minimum volume of deionized water and then poured onto the silica support before being degassed under vacuum, at room temperature. First, a solution of cobalt nitrate (0.8 g of $(Co(NO_3)_2{\cdot}6H_2O)$ in 1.2 mL of water at pH = 2) was poured onto silica and left for 1 h before being dried at 65 °C. After drying, a solution of potassium ferrihexacyanate (0.29 g of $(K_3Fe(CN)_6)$ in 0.8 g H_2O at pH 2) was impregnated and let to react for one day. The initial metal ratio Co/Fe was equal to 1.5 in order to ensure that all ferricyanate groups could react. The silica was washed with deionized water and dried at 65 °C.

Nanocomposite prepared by a one-pot method (sample C). In a typical preparation of PB-MSU (Si/surfactant = 20, Si/Co = 15, Co/Fe = 1.6), a 0.1 M solution of Brij 98 was prepared by dissolution of 5.7 g of surfactant in 50 ml of deionized water at pH 2 followed by the addition of 20.5 g of TEOS (0.098 mol) and 1.91 g (0.0065 mol) of $Co(NO_3)_2{\cdot}6H_2O$. These were slowly dispersed in this solution under magnetic stirring until the solution became perfectly clear. This solution was poured in a rotovapor and 50 wt% of the total mass was removed by evaporation at moderate temperature (30–40 °C) under dynamic vacuum. 1.3 g of $K_3Fe(CN)_6$ (0.0039 mol) (dissolved in the minimum amount of water and Co/Fe = 1.5) was further added to this concentrated solution. The evaporation was continued to completion and the solid was recovered and dried overnight at 65 °C. The material was left as-synthesized since the residual organics cannot disturb the magnetic properties. Besides, they can help to protect the molecular magnets from being affected by the external environment. After reaction, EDAX analysis led to an average composition of $\{Co_3[Fe_2(CN)_6]_2\}_{0.07}{\cdot}MSU_{0.93}$ (embedded surfactants not included). The average weight percentage of surfactants trapped in the silica is 40 wt%.[10] Sample C was treated by HF etching to dissolve silica, which allowed recovery of the nanoparticles alone. This later sample was named C′.

Nanocomposite prepared by simple impregnation of a Co-doped silica (sample D). First, Co-MSU was synthesised using the one-pot method previously described until Co-doped silica was obtained that was filtered off, dried and calcined at 450 °C. Second, 0.22 g of $K_3Fe(CN)_6$ (Co/Fe = 1.5) was dissolved in an appropriate volume of deionized water at pH = 2) and was impregnated into to the Co-silica at room temperature under vacuum.

All preparations (B–D) exhibit an intense dark purple colour.

Instrumentation

X-Ray diffraction was performed in transmission mode using 1 mm Lindemann capillaries on a laboratory SAXS apparatus equipped with a 4 kW copper rotating anode X-ray source (λ = 1.54 Å) and a multilayer focusing Osmic monochromator giving a high flux (10^8 photons s^{-1}) and punctual collimation, with a 2D Image Plate as detector. Diffraction patterns are reported as a function of the wave vector $Q = 2\pi/d = 4\pi \sin\theta/\lambda$,

 This journal is © The Royal Society of Chemistry and the Centre National de la Recherche Scientifique 2009

Published on 22 September 2009 on http://pubs.rsc.org | doi:10.1039/B9NJ00271E
Downloaded by University of Belgrade on 02 January 2013

where d is the correlation length (also called "d-spacing") for disordered systems.

SEM images were obtained on a Leo 1530 microscope (U. Waterloo, WATLAB) at a EHT of 5 kV with gold-coated samples.

Samples for transmission electron microscopy (TEM) measurements were prepared using extractive replicas or ultramicrotomy techniques and then deposited on copper grids. TEM measurements were carried out at 100 kV with a JEOL 1200 EXII microscope. Magnetic susceptibility data were collected with a Quantum Design MPMS-XL SQUID magnetometer working in the temperature range of 1.8–300 K and the magnetic field range of 0–50 kOe. The data were corrected for the sample holder. FT-IR spectra were recorded by transmission on a Brüker Tensor 27 spectrometer.

Results and discussion

The mesoscopic order of the silica matrix was checked by X-ray diffraction (Fig. 1). The initial diffraction pattern displays only one peak characteristic of the 3D wormhole structure of the MSU-type silica.[10,11] The correlation length between pores is equal to 5.5 nm, which corresponds to the sum of pore diameter plus silica wall thickness.

Both samples B and D obtained by impregnation (in one or two steps) lost their mesoscopic order during the preparation. Sample C obtained by the one-pot method exhibits a well-defined peak at a distance slightly higher than that of pure silica (5.7 instead of 5.5 nm). Unlike sample C, surfactants were washed out from sample A (pure silica), which induces a slight shrinkage of its structure. A stronger scattered intensity is also observed for the nanocomposite C, compared with pure silica. Indeed, pure silica exhibits a more ill-ordered structure resulting from the ethanol washing. The ordered mesostructure of C is confirmed by the TEM observation (Fig. 2).

Infrared (IR) spectral measurements of samples B and D in the region between 2000 and 2200 cm^{-1} exhibit an intense peak at about 2121 cm^{-1} (Fig. 3). This peak is ascribable to CN stretching in the Fe(III)–CN–Co(II) structure. The mode of

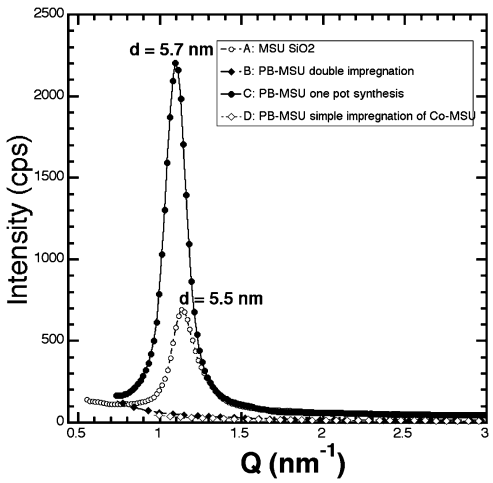

Fig. 1 Powder diffraction patterns obtained for the pure MSU silica (sample A) and the three nanocomposites (B–D); $Q = 2\pi/d$ where d is the correlation length.

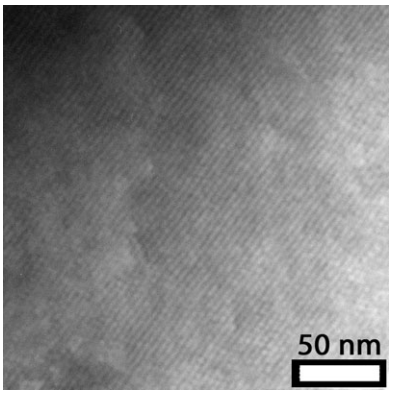

Fig. 2 TEM image of sample C showing the silica ordered mesostructure.

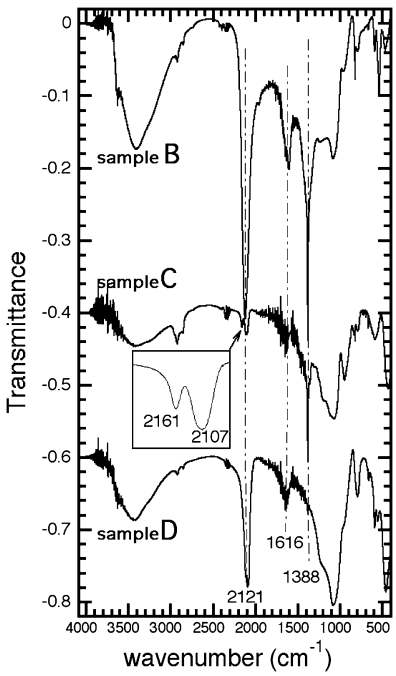

Fig. 3 FT-IR spectra of samples B, C and D (signals have been shifted).

free CN^- ions, initially at ν(CN) = 2080 cm^{-1}, is shifted to higher frequencies when coordinated to metal ions.[6,13] We observe that samples B and D, which exhibit larger crystals (see Fig. 4), exhibit a single intense peak at 2121 cm^{-1}. The IR spectrum of sample C obtained by direct synthesis (as well as for the bulk compound (see Fig. SI 1a, ESI†), reveals a splitting of the CN peaks into two components at 2107 and 2161 cm^{-1}. This splitting cannot be assigned to a mixture between the new compound and unreacted $K_3Fe(CN)_6$ because the latter exhibits a strong narrow peak at 2118 cm^{-1} (Fig. SI 1b, ESI†).

This splitting is not totally understood yet and different explanations have been proposed so far: (i) a possible isomerization with the formation of Co(II)–CN–Fe(III), not expected with our synthesis, or (ii) a partial reduction of Fe(III) in Fe(II) with the formation of Fe(II)–CN–Co(II) bonds.[13,14] Another explanation could be the existence of bridging and dangling

Published on 22 September 2009 on http://pubs.rsc.org | doi:10.1039/B9NJ00271E
Downloaded by University of Belgrade on 02 January 2013

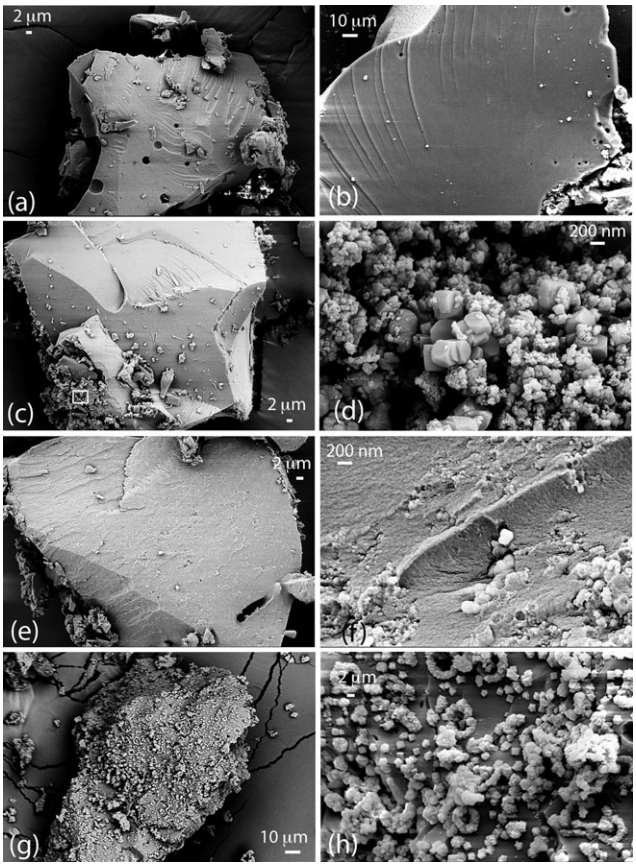

Fig. 4 SEM images of the different mesoporous silicas: A (a, b); B (c, d); C (e, f); D (g, h). The magnification in (d) corresponds to the square in (c).

CN groups due to the formation of small particles since the bulk powder is made of ≈200 nm crystals. The narrow peak at 1388 cm^{-1} is assigned to the stretching mode of nitrate CH_2 groups present in the surfactant cobalt salt, the broad one at 3500 cm^{-1} to OH stretching and that at 1616 cm^{-1} to OH bending. FT-IR analysis of sample C after freeze-drying did not reveal any modification in these components, which proves that water is a structural component of the material.

SEM observation of the four samples (A, B, C, D) is displayed in Fig. 4. The structure of sample A (pure silica) is similar to that reported previously for pure silica obtained by this method, with a monolithic aspect and specific conchoidal fracture.[11] Sample B exhibits a similar structure (Fig. 4(c)) but additional nanocrystals are observed on the particle faces (Fig. 4(d)). EDAX analysis confirmed that the silica matrix does not contain PBA particles and that crystals form mostly in the fractures on the silica monolith (Fig. SI 2, ESI†). Sample C obtained by the co-reaction still exhibits a monolithic structure (Fig. 4(e)) with small particles included in the matrix (Fig. 4(f)). These particles do not exhibit the facetted shapes of pure PBA and EDAX analysis confirms that both the matrix and the particles exhibit the same chemical composition with a rather constant iron and cobalt content (Fig. SI 3, ESI†) with Co/Fe ≈ 1.5. Finally, sample D reveals that the impregnation of silica, which had been impregnated beforehand by cobalt ions and dried, by an aqueous solution of $[Fe(CN)_6]^{3-}$ ions

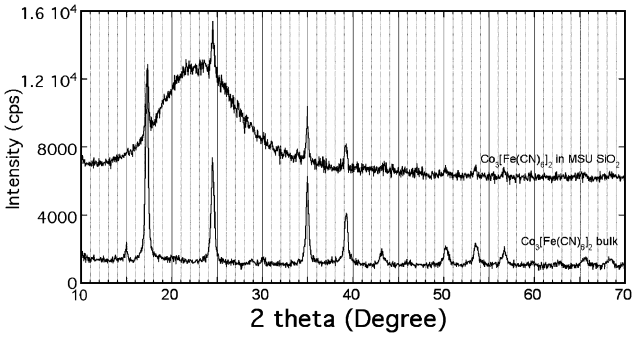

Fig. 5 XRD pattern for a compound synthesised alone (bottom) and for sample C (top).

leads to a partial leakage of cobalt ions that react onto the surface of the silica particles, especially at the aperture of macroporous pores. As a result, rings of crystals are observed around the macropore openings (Fig. 4(g) and (h)).

The X-ray diffraction pattern (Fig. 5) of sample C confirms the existence of a ferricyanide-based crystalline structure for both the bulk synthesis and the synthesis embedded into the silica matrix. Diffraction peaks are similar to those observed previously in $Co_3[(Co(CN)_6]_2$.[14] Their average size is in perfect agreement with the pore diameter expected from the XRD pattern of silica (Fig. 1).

PBA nanoparticles with a mean size value of 3–4 nm can be clearly seen after removal of silica from the nanocomposite material by HF etching (Fig. 6). They are well dispersed and no aggregates are observed.

The magnetic properties of these samples have been studied by dc and ac modes by using a SQUID magnetometer working in the temperature range between 1.8 and 300 K. We report the magnetic measurements of both samples C and C′ obtained after silica dissolution by HF treatment of C. The zero field-cooled (ZFC)/field-cooled (FC) magnetisation curves measured for sample C are displayed in Fig. 7. The ZFC curve was obtained by recording the magnetisation when the sample was heated under a field of 10 Oe after being cooled in zero magnetic field. The FC data were obtained by cooling the sample under the same magnetic field after the ZFC experiment and recording the change in sample magnetisation with temperature. The ZFC and FC curves reveal different

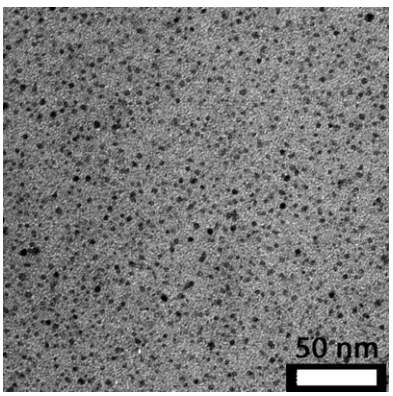

Fig. 6 TEM image of the cyano-bridged coordination polymer nanoparticles (C′) obtained after HF etching of sample C.

 This journal is © The Royal Society of Chemistry and the Centre National de la Recherche Scientifique 2009

Published on 22 September 2009 on http://pubs.rsc.org | doi:10.1039/B9NJ00271E
Downloaded by University of Belgrade on 02 January 2013

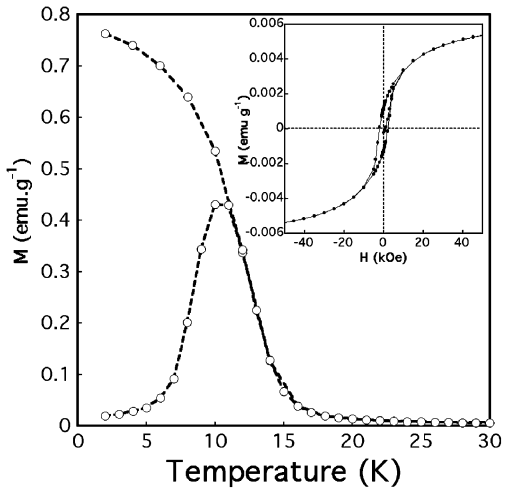

Fig. 7 Field-cooled and zero field-cooled magnetisation (FC/ZFC) *vs*. temperature curves performed with an applied field of 10 Oe for the sample C. Inset: Field dependence of the magnetisation for the sample C performed at 2 K.

behaviours: the ZFC curve exhibits a maximum at T_{max} = 10.51 K while the FC curve increases as the temperature decreases and tends to saturation at low temperature. Both curves coincide at high temperatures and begin to separate at T_{sep} = 11.30 K. The FC/ZFC curves performed for the sample C′ after removing silica from C by HF etching, shows very similar irreversible behaviour with a maximum on the ZFC curve observed at 10.80 K (Table 1).

The field dependence of the magnetisation performed at 2 K for samples C and C′ shows that saturation magnetisation at 50 kOe is equal to 5.34 and 35.13 emu g^{-1} for C and C′, respectively.

The last value corresponds to a value of 3.7 μ_B, relative to the following molecular formula: $Co_3[Fe(CN)_6]_2$ (Co/Fe = 1.5 compared with the initial value of 1.6). This value is in agreement with the value of 3.5 μ_B calculated for the $\{Co_3Fe_2\}$ unit with antiferromagnetic Co^{2+}–Fe^{3+} interactions through the cyano bridges. The value of the saturation magnetisation of 5.34 emu g^{-1} observed for the sample C corresponds to a total amount of 15.2 wt% of nanoparticles into the silica. The EDAX analysis gave an atomic ratio (Fe + Co)/Si of 22 wt%. Taking into account the existence of 40 wt% of surfactant in the as-synthesized material, we obtain a total amount of 13 wt% of nanoparticles, in good agreement with the magnetic measurements. Both samples (C and C′) exhibit a hysteresis effect with a coercive field of 2.0 and 1.98 kOe, respectively (inset of Fig. 6 and Table 1).

In order to determine the magnetic regime of the nanoparticles, alternating current (ac) susceptibility measurements have been performed. The temperature dependence of the in-phase, χ' (absorptive), and out-of-phase, χ'' (dispersive), components of the ac susceptibility measured in zero static field for frequencies varying from 1 Hz to 1488 Hz for the sample C are shown in Fig. 8. At 1 Hz, both χ' and χ'' responses present a peak at 11.9 and 11.3 K, respectively. These peaks shift toward higher temperatures as the frequency increases. The sample C′ (nanoparticles alone) shows the same frequency dependent behaviour as C, with χ' and χ'' peaks at 11.5 and 11.0 K at 1 Hz. Such frequency-dependent behaviour is characteristic of the presence of nanoparticles of cyano-bridged coordination polymer presenting short range magnetic ordering.[15,16] The magnetic transition observed at

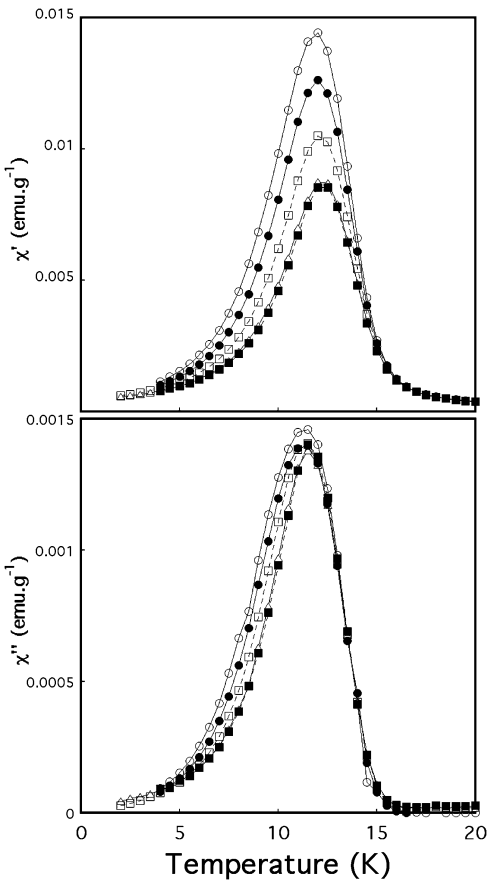

Fig. 8 Temperature dependence of (top) in-phase, χ', and (bottom) out-of-phase, χ'', components of the ac susceptibility performed in zero field for the sample C. Frequencies: 1 Hz (○), 9.99 Hz (●), 125 Hz (□), 998 Hz (■) and 1498 Hz (△).

Table 1 Magnetic data for samples C, C′ and B

		Arrhenius law[a]		Vogel–Fulcher law			Power law				
Sample	T_{max}/K	(E_a/k_B)/K	τ_0/s	T_g/K	τ_0/s	(E_a/k_B)/K	T_g/K	τ_0/s	zv	T_g/K AT line	H_c/kOe
C	10.51	2589	1.92×10^{-88}	10.33	1.74×10^{-12}	23.2	11.75	1.86×10^{-13}	6.9	9.65	2.00
C′	10.80	2115	3.42×10^{-82}	10.0	1.44×10^{-12}	35.2	11.4	2.17×10^{-13}	8.2	11.02	1.98
B	10.92	1262	1.21×10^{-52}	8.9	2.6×10^{-12}	45.6	11.8	2.65×10^{-10}	10	10.1	1.04

[a] Obtained at the maximum of the ZFC curve.

Published on 22 September 2009 on http://pubs.rsc.org | doi:10.1039/B9NJ00271E
Downloaded by University of Belgrade on 02 January 2013

low temperature may be attributed to three limiting cases: (i) the blocking process of isolated or weakly interacting superparamagnetic nanoparticles usually well described with an Arrhenius law;[17] (ii) nano-cluster-glass-like transition caused by strong magnetostatic interparticle interactions and by randomness,[18] or (iii) intraparticle spin glass-like regime due to the particle surface spin disorder.[6]

First of all, the temperature dependence of the relaxation time extracted from the maximum of the χ'' component of the ac susceptibility was fitted with an Arrhenius law:

$$\tau = \tau_0 \exp(E_a/k_B T) \quad (1)$$

where E_a is the average energy barrier for the reversal of the magnetisation, τ_0 is the attempt time and k_B is the Boltzmann constant. The values of the energy barrier, E_a/k_B, are equal to 2589 and 2115 K for C and C′, respectively, and the values of pre-exponential factor, τ_0, are equal to 1.92×10^{-88} and 3.42×10^{-82} s (Fig. 8). Usual values of τ_0 observed for superparamagnetic systems are in the range of 10^{-8}–10^{-12} s. Hence, these low values have no physical meaning and they may be interpreted as the signature of a correlation among magnetic moments introduced by strong magnetostatic interparticle interactions. The probable presence of these interactions can be probed by the temperature dependence of the relaxation time. This evolution was fitted with the Vogel–Fulcher law commonly used for magnetically interacting clusters:[19]

$$\tau = \tau_0 \exp(E_a/k_B(T - T_0)) \quad (2)$$

In comparison with the Arrhenius law adopted for isolated nanoparticles, the interparticle interactions deduced from this analysis, are introduced by means of an additional parameter, T_0. The best fits for sample C (C′) give satisfactory parameters of E_a/k_B, τ_0 and T_0 equal to 23.2 (35.2) K, 1.74×10^{-12} (1.44×10^{-12}) s and 10.33 (10.0) K (Table 1), suggesting the presence of relatively strong interparticle interactions in both cases (Fig. 9(a)).

In order to verify if the dynamics in these systems exhibit critical slowing down as usually observed in canonical spin-glass systems presenting strong interparticle interactions, we used the critical scaling law of the spin dynamics:

$$\tau = \tau_0[T_g/(T_{max} - T_g)]^{zv} \quad (3)$$

where T_g ($\neq 0$) is the glass temperature, f is the frequency and zv is a critical exponent.[20] For the sample C (C′), the best fits gives the following parameters, T_g = 11.75 (11.40) K, τ_0 = 1.86×10^{-13} (2.17×10^{-13}) s and zv = 6.9 (8.2) (Fig. 9(b), Table 1). The obtained zv as well as the τ_0 values are perfectly in the range 4–12 and $\sim 10^{-13}$ s, respectively, expected for classical spin glass systems.

In order to verify if the samples C and C′ present a spin-glass regime, the temperature dependences of the ac susceptibility at 125 Hz were measured with different applied direct current (dc) fields (Fig. 9). For both samples, the peak intensity of the two components χ' and χ'' decreases as the field increases. This had been observed previously for cyano-bridged coordination polymer nanoparticles stabilised by capping ligands in organic solvents.[20]

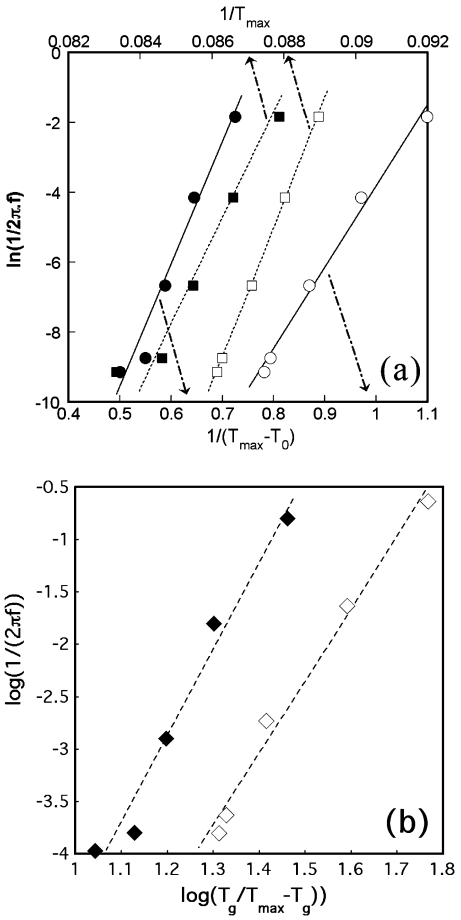

Fig. 9 (a) Thermal variations of the relaxation time according to the Arrhenius law, $\tau = \tau_0 \exp(E_a/k_B T)$, (□) and the Vogel–Fulcher law, $\tau = \tau_0 \exp(E_a/k_B(T - T_0))$, (○) for sample C and according to the Arrhenius law, $\tau = \tau_0 \exp(E_a/k_B T)$, (■) and the Vogel–Fulcher law, $\tau = \tau_0 \exp(E_a/k_B(T - T_0))$, (●) for sample C′. (b) Thermal variation of the relaxation time according to a power law, $\tau = \tau_0[T_g/(T_{max} - T_g)]^{zv}$, for C (◇) and C′ (◆).

The trace of the temperature maxima of the χ' and χ'' components as a function of $H^{2/3}$ gives linear dependence that corresponds to the so-called de Almeida–Thouless (AT) line.[21] It is given by the equation:

$$H \propto (1 - (T_{max}/T_f))^{3/2} \quad (4)$$

The spin-glass transition temperature obtained by extrapolation of the AT line back to $H = 0$ was found equal to 9.65 K and 11.02 K for C and C′, respectively (Fig. 10). These values are relatively close to the T_{max} values obtained by the maximum on the ZFC curve, equal to 10.51 K. Usually, the compliance of the data with the AT line is considered to be an evidence for the existence of a spin-glass behaviour.[22]

To summarise, all parameters extracted from this magnetic study indicate the presence of strong magnetostatic intra-particle interactions that induce a spin-glass regime. It is worth noting that previously published cyano-bridged coordination polymer nanoparticles obtained in mesostructured silica by step-by-step coordination of precursors were isolated from each other and did not exhibit magnetostatic interactions.[3] On the other hand, the presence of a surface spin frustration

 This journal is © The Royal Society of Chemistry and the Centre National de la Recherche Scientifique 2009

Published on 22 September 2009 on http://pubs.rsc.org | doi:10.1039/B9NJ00271E
Downloaded by University of Belgrade on 02 January 2013

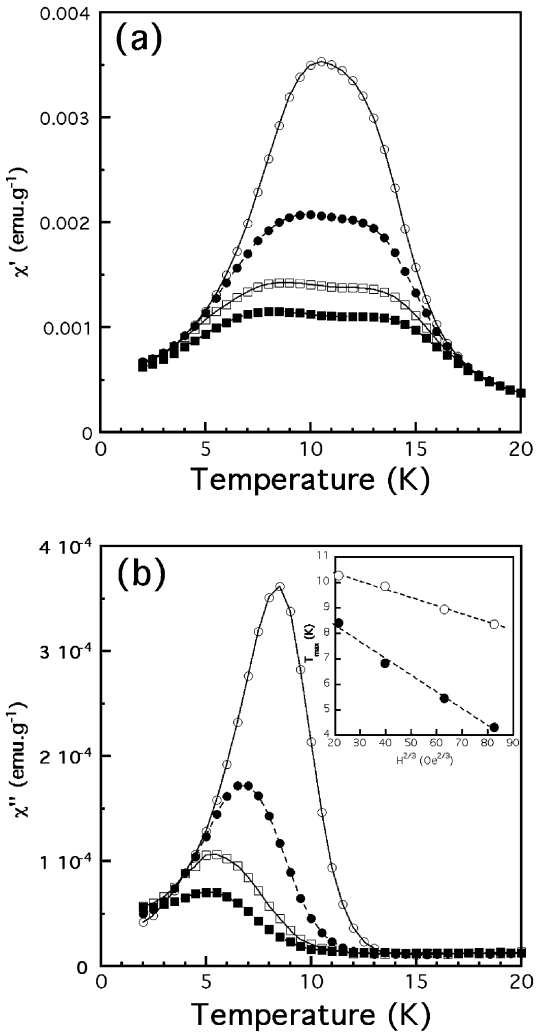

Fig. 10 Temperature dependence of (top) in-phase, χ' and (bottom) out-of-phase, χ'', components of the ac susceptibility. Applied field: 100 Oe (○); 250 Oe (●), 500 Oe (□) and 750 Oe (■). Inset: T_{max} (χ'') is plotted against $H^{2/3}$ for the variation of the (top) χ' and (bottom) χ'' parts of the ac susceptibility performed with different applied fields for sample C in silica matrix (●) and after the silica was removed by HF treatment (○). The solid lines show a linear fit to the data.

induced by the interactions of nanoparticles with the silica matrix has been assumed. In the present case, it is evident that the magnetostatic interactions are predominant; however, we cannot completely exclude also an influence of the particles surface spin disorder, which can also contribute to modify the superparamagnetic regime of the nanoparticles.

The magnetic properties of the sample B are similar to what is observed for sample C. The FC/ZFC curves also present irreversibility and the maximum temperature on the ZFC curve is observed at 10.9 K (Table 1 and Fig. SI 4, ESI†). The temperature dependence of the ac susceptibility, its in-phase, χ', and its out-of-phase, χ'', components measured in zero static field show a frequency dependence suggesting the presence of a short range magnetic ordering. The Arrhenius fit of the thermal variation of the relaxation time shows a very small value of the parameter $\tau_0 = 1.21 \times 10^{-52}$ s, which has no physical meaning, while the Vogel–Fulcher fit shows the presence of strong interparticle interactions (Table 1). This conclusion was confirmed by the power law $\tau = \tau_0[T_g/(T_{max} - T_g)]^{z\nu}$ fitting of the temperature dependence of the relaxation time giving satisfactory parameters of T_g = 11.8 K, $\tau_0 = 2.65 \times 10^{-10}$ s and $z\nu = 10$ (Table 1) usually observed for the strongly interacted nanoparticles presenting spin-glass behaviour such as the sample C. As for sample D, the FC/ZFC curves as well as the temperature dependence of the ac susceptibility show no peak in the temperature region 1.8–300 K showing that visibly no cyano-bridged $Co^{2+}/[Fe(CN)_6]^{3-}$ is present.

Conclusions

We successfully synthesised nanoparticles of Prussian Blue analogues by a direct method based on integrative chemistry where the synthesis of the particles, $Co_3[Fe(CN)_6]_2$, and of the confinement matrix (MSU-type mesostructured silica) are run in parallel. This method allowed us to obtain a composite structure with a homogeneous dispersion of a high amount of PBA nanoparticles (around 15%) with an average size ranging between 2 and 4 nm. Magnetic measurements confirmed the occurrence of this reaction and revealed a strong magnetostatic component due to interparticle interactions. This synthesis, which does not require any pre-grafting step, is currently applied to a larger family of Prussian Blue analogues.

References

1 O. Kahn, *Philos. Trans. R. Soc. London, Ser. A*, 1999, **357**, 3005; M. Verdaguer, A. Bleuzen, V. Marvaud, J. Vaissermann, M. Seuleiman, C. Desplanches, A. Scuiller, C. Train, R. Garde, G. Gelly, C. Lomenech, I. Rosenmann, P. Veillet, C. Cartier dit Moulin and F. Villain, *Coord. Chem. Rev.*, 1999, **190–192**, 1023; O. Kahn, *Acc. Chem. Res.*, 2000, **33**, 647; M. Verdaguer, *Polyhedron*, 2001, **20**, 1115; O. Hatlevik, W. E. Buschmann, J. Zhang, J. L. Manson and J. S. Miller, *Adv. Mater.*, 1999, **11**, 914; S. M. Holmes and G. S. Girolami, *J. Am. Chem. Soc.*, 1999, **121**, 5593; B. G. Morin, C. Hahm, A. J. Epstein and J. S. Miller, *J. Appl. Phys.*, 1994, **75**, 5782; J. S. Miller, *Adv. Mater.*, 1994, **6**, 322; S. Ferlay, T. Mallah, R. Ouahès, P. Veillet and M. Verdaguer, *Inorg. Chem.*, 1999, **38**, 229; W. E. Buschmann, S. C. Paulson, C. M. Wynn, M. Girtu, A. J. Epstein, H. S. White and J. S. Miller, *Adv. Mater.*, 1997, **9**, 645; W. R. Entley and G. S. Girolami, *Science*, 1995, **268**, 397; S. Ferlay, T. Mallah, R. Ouahes, P. Veillet and M. Verdaguer, *Nature*, 1995, **378**, 701; V. Gadet, T. Mallah, I. Castro and M. Verdaguer, *J. Am. Chem. Soc.*, 1992, **114**, 9213; T. Mallah, S. Thiebaut, M. Verdaguer and P. Veillet, *Science*, 1993, **262**, 1554; O. Sato, T. Iyoda, A. Fujishima and K. Hashimoto, *Science*, 1996, **271**, 49; S. Ohkoshi and K. Hashimoto, *J. Am. Chem. Soc.*, 1999, **121**, 10591.
2 S. Vaucher, M. Li and S. Mann, *Angew. Chem., Int. Ed.*, 2000, **39**, 1793.
3 L. Catala, T. Gacoin, J.-P. Boilot, E. Riviere, C. Paulsen, E. Lhotel and T. Mallah, *Adv. Mater.*, 2003, **15**, 826.
4 T. Uemura and S. Kitagawa, *J. Am. Chem. Soc.*, 2003, **125**, 7814; L. Catala, A. Gloter, O. Stephan, G. Rogez and T. Mallah, *Chem. Commun.*, 2006, 1018; D. Brinzei, L. Catala, C. Mathonière, W. Wensdorfer, A. Gloter, O. Stephan and T. Mallah, *J. Am. Chem. Soc.*, 2007, **129**, 3778; J. M. Domíngez-Vera and E. Colacio, *Inorg. Chem.*, 2003, **42**, 6983.
5 G. Clavel, J. Larionova, Y. Guari and Ch. Guérin, *Chem.–Eur. J.*, 2006, **12**, 3798; J. Larionova, Y. Guari, H. Sayegh and Ch. Guérin, *Inorg. Chim. Acta*, 2007, **360**, 3829; Y. Guari, J. Larionova, C. Blanc, P. Dieudonné, A. Tokarev and C. Guérin, *Langmuir*, 2009, **25**, 1138.

View Article Online

6 B. Folch, Y. Guari, J. Larionova, C. Luna, C. Sangregorio, C. Innocenti, A. Caneschi and C. Guérin, *New J. Chem.*, 2008, **32**, 273.
7 H. Yang and D. Zhao, *J. Mater. Chem.*, 2005, **15**, 1217; J. J. Baumberg, *Nat. Mater.*, 2006, **5**, 2.
8 R. Backov, *Soft Matter*, 2006, **2**, 452; E. Prouzet, S. Ravaine, C. Sanchez and R. Backov, *New J. Chem.*, 2008, **32**, 1284.
9 C. Boissière, A. Larbot, C. Bourgaux, E. Prouzet and C. A. Bunton, *Chem. Mater.*, 2001, **13**, 3580.
10 S. A. Bagshaw, E. Prouzet and T. J. Pinnavia, *Science*, 1995, **269**, 1242; C. Boissière, A. Larbot, A. van der Lee, P. J. Kooyman and E. Prouzet, *Chem. Mater.*, 2000, **12**, 2902; E. Prouzet and C. Boissière, *C. R. Chim.*, 2005, **8**, 579.
11 D. O. de Zárate, F. Bouyer, H. Zschiedrich, P. J. Kooyman, Ph. Trens, J. Lapichella, R. Durand, C. Guillem and E. Prouzet, *Chem. Mater.*, 2008, **20**, 1410.
12 A. Bleuzen, C. Lomenech, V. Escax, F. Villain, F. Varret, C. Cartier dit Moulin and M. Verdaguer, *J. Am. Chem. Soc.*, 2000, **122**, 6648; O. Sato, Y. Einaga, Y. Iyoda, A. Fujishima and K. Hashimoto, *J. Phys. Chem. B*, 1997, **101**, 3903; D. F. Shriver and D. B. Brown, *Inorg. Chem.*, 1969, **8**, 42.
13 E. Reguera, J. F. Bertran, C. Diaz, J. Bianco and S. Rondon, *Hyperfine Interact.*, 1990, **53**, 391.
14 D. H. M. Buchold and C. Feldmann, *Chem. Mater.*, 2007, **19**, 3376.
15 J. Larionova, Y. Guari, C. Sangregorio and C. Guérin, *New J. Chem.*, 2009, **33**, 1177.
16 L. Néel, *Ann. Geophys.*, 1949, **60**, 661; J. L. Dormann, L. Bessais and D. Fiorani, *J. Phys. Chem. C*, 1988, **21**, 2015.
17 J. A. Mydosh, *Spin Glasses*, Taylor and Francis, Washington DC, 1993.
18 C. Djurberg, P. Svedlindh, P. Nordblad, M. F. Hansen, F. Bodker and S. Morup, *Phys. Rev. Lett.*, 1997, **79**, 5154; G. Balaji, G. Wilde, J. Weissmuller, N. S. Gabhiye and V. K. Sankaranarayanan, *Phys. Status Solidi B*, 2004, **241**, 1589.
19 J. A. Mydosh, *Phys. Rev. B: Condens. Matter Mater. Phys.*, 1989, **40**, 11243.
20 E. Chelebaeva, Y. Guari, J. Larionova, A. Trifonov and C. Guérin, *Chem. Mater.*, 2008, **20**, 1367.
21 J. R. L. Almeida and D. J. Thouless, *J. Phys. A: Math. Gen.*, 1978, **11**, 983.
22 T. Jonsson, J. Mattsson, C. Djurberg, F. A. Khan, P. Nordblad and P. Svedlindh, *Phys. Rev. Lett.*, 1995, **75**, 4138.

Published on 22 September 2009 on http://pubs.rsc.org | doi:10.1039/B9NJ00271E
Downloaded by University of Belgrade on 02 January 2013

 This journal is © The Royal Society of Chemistry and the Centre National de la Recherche Scientifique 2009